TECHNISCHE UNIVERSITÄT
KAISERSLAUTERN

SCHRIFTEN ZUR

FUNKTIONALANALYSIS
UND GEOMATHEMATIK

W. Freeden, M. Schreiner

Biorthogonal Locally Supported Wavelets on the Sphere Based on Zonal Kernel Functions

Bericht 27 – Oktober 2006

FACHBEREICH MATHEMATIK

Biorthogonal Locally Supported Wavelets on the Sphere Based on Zonal Kernel Functions

by

Willi Freeden
University of Kaiserslautern
Geomathematics Group
P.O. Box 3049
67653 Kaiserslautern
Germany
Email: freeden@mathematik.uni-kl.de

Michael Schreiner
University of Buchs NTB
Laboratory for Industrial Mathematics
Werdenbergstrasse 4
CH–9471 Buchs
Switzerland
Email: schreiner@ntb.ch

This paper presents a method for approximating spherical functions from discrete data of a block–wise grid structure. The essential ingredients of the approach are scaling and wavelet functions within a biorthogonalisation process generated by locally supported zonal kernel functions. In consequence, geophysically and geodetically relevant problems involving rotation–invariant pseudodifferential operators become attackable. A multiresolution analysis is formulated enabling a fast wavelet transform similar to the algorithms known from one–dimensional Euclidean theory.

AMS-Classification: 42C40, 43A90, 65T60

Keywords: Spherical Multiresolution Analysis, Zonal Kernel Functions , Biorthogonalisation, Decomposition and Reconstruction Schemes, Fast Wavelet Transform.

1 Introduction

Spherical wavelets are used as mathematical tool for breaking up a complicated structure of a function into many simple pieces at different scales and positions. In the last years, wavelets on the sphere have been in the focus of several research groups which led to different wavelet approaches. Common to all these proposals is a multiresolution analysis which enables a balanced amount of both frequency (more accurately, angular momentum) and space localization.

In the year 1995, a (parametric) concept of spherical wavelets was proposed by Dahlke, Dahmen, Schmitt, and Weinreich (see [5] and [29]) based on a tensor product basis, in which one component is a spline of exponential (E-) type. The so–called E-splines provide not only $C^{(1)}$–wavelets, but also guarantee the reproduction of trigonometric functions within the wavelet expansion. Potts and Tasche [24] form tensor products of interpolatory trigonometric wavelets and polynomial wavelets in accordance with a usual longitude/lattitude parametrization of the sphere. These wavelets satisfy the $C^{(1)}$–assumption described in [29] only in an approximate sense. Another multiresolution tensor spline method on the sphere is proposed by Lyche and Schumaker [23]. Starting with a triangulation of the sphere, Schröder and Sweldens [28] construct spherical Haar–type wavelets on the triangles yielding smoother wavelets by virtue of the so–called lifting scheme. A group theoretical approach to a continuous wavelet transform on the sphere is followed by Antoine [1], [2] and Holschneider [21]. The parameter choice of their continuous wavelet transform is the product of $SO(3)$ (for the motion on the sphere) and $\mathbb{R}^+$ (for the dilations). A continuous wavelet transform approach for analyzing functions on the sphere is presented by Dahlke and Maass [6].

The constructions of the Geomathematics Group in Kaiserslautern ([15], [19], [20], [8], [9], [11], [12]) are intrinsically based on the specific properties concerning the geometry of the sphere and the theory of 'spherical polynomials', i.e., in the jargon of the geosciences 'spherical harmonics'. Two approaches to spherical wavelets have been established: On the one hand, a continuous wavelet transform (and its discretizations) was obtained by taking particular advantage of the conception of spherical singular integrals. Within this framework the wavelets turn out to be kernel functions generated by summing up certain clusters of spherical harmonic expressions. The wavelets are definable either by increasing space localization of the kernels or by decreasing frequency localization of their corresponding symbols (i.e., Fourier transform in terms of spherical harmonics). Wavelet modeling is provided by a two–parameter family reflecting the different levels of localization and resolution. On the other hand the authors [16], [8] presented a scale discrete wavelet transform involving band–limited as well as non–band–limited kernel representations by forming the so–called P–scale or M–scale wavelet representations. With the help of approximate or exact (for spherical harmonic or spherical splines) interpolatory formulae all wavelet transforms allow fully discrete approximants via tree algorithms (i.e., pyramid schemes) [25], [8], [7], [4], [10], [13], [3]. Recently, a multiresolution analysis based on zonal functions with a local support has been developed by the authors of this paper (see [18] and the references therein).

Looking at the different concepts, two essential approaches can be identified: The first one uses certain grids on the sphere and tries to transfer concepts of the one–dimensional wavelet

analysis to the sphere. The approaches with longitude/latitde grids or triangulations fall into this category. The second approach put the emphasis on the solution of rotation–invariant pseudodifferential equations on the sphere (as proposed, e.g., in [8]). For this concept, zonal functions are an appropriate tool. In this case, there is — at first glance — no need for a particular point distribution on the sphere.

In this paper we are interested in a new compromise for the construction of spherical wavelets. In fact, our wavelets are based on zonal functions but also relate to structured grids in order to obtain fast algorithms that are easy to implement.

The key points of our paper can be characterized as follows:

- The wavelets and the scaling function are based on zonal kernel functions so that our approach is well–suited for the solution and regularization of rotation–invariant pseudo-differential equations.
- The wavelets are locally supported so that the integration can be made efficient.
- The construction is based on a biorthogonal system of zonal functions, which gives us almost all advantages of an orthogonal approach.
- A new block–wise grid structure is used on the sphere: The points lie on circles of constant latitude to ensure that the construction of a biorthogonal system is not expensive. But the grid gets sparser in the polar regions so that there are not too large differences in the distances between neighboring points.
- The grid is organized in blocks of size 2^p by 2^{p-1} so that the algorithms can be formulated easily.
- Finally, a scaling equation is established with only a few coefficients. In fact, we end up with a fast wavelet transform which is completely similar to the algorithms known from one–dimensional Euclidean wavelet theory.

What is the prize that we have to pay for all these advantages? It is by no means dramatic: First, we do not develop a multiresolution analysis of the whole space of square–integrable functions but on finite dimensional subspaces. In fact, we have – at the beginning of the analysis — to choose a finest level of resolution. From numerical point of view, this is what has to be done for practical applications, anyway. Second, we use zonal kernel functions only at the finest scale. On the coarser levels, the wavelets and the scaling functions turn out to be linear combinations of zonal kernel functions centered at different points. But this does not influence the applicability to the solution of rotation–invariant pseudodifferential equations on the sphere, since the isotropy is observed on the finest level and all other information originated on this level is transported automatically to the coarser ones.

Since our work is rather technical, we would like to motivate one of the main ideas right now: Consider four points of a structured grid, where four zonal functions $\varphi_{ij}^{(0)}$, $i, j \in \{0, 1\}$ are

centered. This is the scaling function at scale 0, i.e., at the finest scale. Going to the coarser scale we are led from these four functions to the scaling function $\varphi_{00}^{(1)}$ at scale 1 together with three wavelets:

$$\begin{aligned}
\varphi_{00}^{(1)} &= \frac{1}{2}\left(\varphi_{00}^{(0)} + \varphi_{10}^{(0)} + \varphi_{01}^{(0)} + \varphi_{11}^{(0)}\right) \\
{}_{EW}\psi_{00}^{(1)} &= \frac{1}{2}\left(\varphi_{00}^{(0)} - \varphi_{10}^{(0)} + \varphi_{01}^{(0)} - \varphi_{11}^{(0)}\right) \\
{}_{NS}\psi_{00}^{(1)} &= \frac{1}{2}\left(\varphi_{00}^{(0)} + \varphi_{10}^{(0)} - \varphi_{01}^{(0)} - \varphi_{11}^{(0)}\right) \\
{}_{D}\psi_{00}^{(1)} &= \frac{1}{2}\left(\varphi_{00}^{(0)} - \varphi_{10}^{(0)} - \varphi_{01}^{(0)} + \varphi_{11}^{(0)}\right)
\end{aligned}$$

Figure 1 sketches this construction. The wavelets can be associated with a certain direction for the analysis: east–west (EW), north–south (NS), and diagonal (D). Thus, for scale 1 and all larger scales the functions are not zonal, anymore.

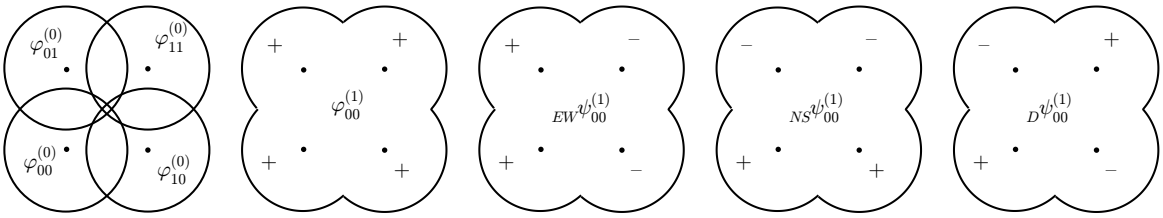

Figure 1: Out of 4 neighboring scaling functions at scale 0 the scale function at scale 1 as well as 3 wavelets (with directional information) are built.

The paper is organized as follows: In Chapter 2 we show the construction of the block grids. Chapter 3 introduces the scaling functions, that are used in Chapter 4 for the definition of the wavelets. The multiresolution analysis together with the fast wavelet transform is discussed in Chapter 5. Some examples are shown in Chapter 6. At the end, we summarize our results.

2 Block Grids

Our approach to spherical wavelets is strongly related to grids on the sphere with a particular structure. In what follows, we describe the construction of such grids. Our whole procedure is done on one half of the northern hemisphere of the unit sphere Ω in three–dimensional Euclidean space $\mathbb{R}^3$. For the other parts of the sphere the grid is formed similarly in a symmetric manner.

The main concepts are as follows: The distances between neighboring points in the grid should not be too different. A coarsening of the grid should be possible. The generation of a biorthogonal function system out of zonal kernel functions centered at the grid points should be easy (for the Euclidean case see, e.g., the investigations in [22]). These requirements lead us

to a construction, where the grid points are lying on circles of latitude, and where the points are organized block–wise, such that in each block there are 2^p times 2^{p-1} grid points.

Let us fix an integer $N \geq 2$, that defines the finest level of the grid. We set

$$\Delta\lambda = \pi 2^{-(N+1)}$$

and

$$\lambda_i = i\Delta\lambda,\ i = 0, \ldots, 2^{N+1} - 1. \tag{1}$$

For the north–south direction, we assume that the values ϑ_i, $i = 0, \ldots, 2^N - 2$ are ordered in the following way

$$\frac{\pi}{2} > \vartheta_0 > \ldots > \vartheta_{2^N-2} > 0. \tag{2}$$

The points η_{ij} on the unit sphere Ω are then defined by

$$\eta_{ij} = \begin{pmatrix} \sin\vartheta_j \cos\lambda_i \\ \sin\vartheta_j \sin\lambda_i \\ \cos\vartheta_j \end{pmatrix}, \quad i = 0, \ldots, 2^{N+1} - 1,\ j = 0, \ldots, 2^N - 2. \tag{3}$$

Not all of the point η_{ij} are used during our work. The grid is block–wise organized. From scale to scale the number of points is reduced. The details will be explained in the following lines.

For the scale $l = 0$ we define the index sets ($k = 0, \ldots, N-1$) as follows:

$$\mathcal{I}_k^{(0)} = \left\{ (i,j) \;\middle|\; i = 0(2^k)2^N - 2^k,\ j = 2^N - 2^{N-k}(1)2^N - 2^{N-k-1} - 1 \right\}. \tag{4}$$

(Throughout the paper, we write $i = a(b)c$ for the set of indices $i = a, a+b, a+2b, \ldots, c$). As an example we consider the scale $l = 0$ in Figure 2, where we have listed the index sets for the case $N = 3$.

Scale	Set	i	j
$l = 0$	$\mathcal{I}_0^{(0)}$	$0, 1, 2, \ldots, 7$	$0, 1, 2, 3$
	$\mathcal{I}_1^{(0)}$	$0, 2, 4, 6$	$4, 5$
	$\mathcal{I}_2^{(0)}$	$0, 4$	6
$l = 1$	$\mathcal{I}_0^{(1)}$	$0, 2, 4, 6$	$0, 2$
	$\mathcal{I}_1^{(1)}$	$0, 4$	4
	$\mathcal{I}_2^{(1)}$	0	6
$l = 2$	$\mathcal{I}_0^{(2)}$	$0, 4$	0
	$\mathcal{I}_1^{(2)}$	0	4
$l = 3$	$\mathcal{I}_0^{(3)}$	0	0

Figure 2: Index sets for the case $N = 3$

Going from scale to scale, the number of indices in each set is reduced by a factor 2 both for i and j. In more detail, for the scale l, we set for $k = 0, \ldots, N - l - 1$

$$\mathcal{I}_k^{(l)} = \left\{ (i,j) \;\middle|\; i = 0(2^{k+l})2^N - 2^{k+l},\ j = 2^N - 2^{N-k}(2^l)2^N - 2^{N-k-1} - 2^l \right\}. \tag{5}$$

A special situation occurs, if $k = N - l$ (for $l > 0$). In this case the index set $\mathcal{I}_k^{(l)}$ would be empty using the formula of the definition stated above. This is the reason why we set

$$\mathcal{I}_{N-l}^{(l)} = \left\{ (i,j) \;\middle|\; i = 0,\ j = 2^N - 2^l \right\}. \tag{6}$$

By definition, all other $\mathcal{I}_k^{(l)}$ are set to $\mathcal{I}_k^{(l)} = \emptyset$. In addition, we let $\mathcal{I}^{(l)} = \bigcup_{k=0}^{N-l} \mathcal{I}_k^{(l)}$.

For given N, we have therefore defined the following non empty sets: $\mathcal{I}_0^{(0)}, \ldots, \mathcal{I}_{N-1}^{(0)}$, $\mathcal{I}_1^{(1)}, \ldots,$ $\mathcal{I}_{N-1}^{(1)}$, $\mathcal{I}_1^{(2)}, \ldots, \mathcal{I}_{N-2}^{(2)}$, …, $\mathcal{I}_0^{(N)}$. Figure 2 shows an example for $N = 3$.

In accordance with our construction the total number of indices in the sets amounts to

$$\#\mathcal{I}_k^{(l)} = 2^{2N-2l-2k-1},\ k = 0, \ldots, N - l - 1,\ l = 0, \ldots, N, \tag{7}$$

and

$$\#\mathcal{I}_{N-l}^{(l)} = 1,\ l = 1, \ldots, N. \tag{8}$$

Thus it readily follows that (with δ_{lj} denoting the Kronecker symbol)

$$\begin{aligned} \#\mathcal{I}^{(l)} &= \frac{1}{2} \sum_{k=0}^{N-l-1} 4^{N-k-l} + (1 - \delta_{l0}) \\ &= 2 \sum_{p=0}^{N-l-1} 4^p + (1 - \delta_{l0}) \\ &= 2\frac{1 - 4^{N-l}}{1 - 4} + (1 - \delta_{l0}) \\ &= \frac{2}{3}(4^{N-l} - 1) + (1 - \delta_{l0}). \end{aligned}$$

For our wavelet approach, two aspects are of importance: First, we start from a point set for the scale $l = 0$ with respect to the index sets and the points η_{ij}. This point set is the extendable to the whole sphere. Second, for all scales, a so–called SGS, i.e., 'scale grid support', with respect to the point set is inherent in the construction. We associate to each kernel functions under consideration a scale–dependent relevant area on the unit sphere Ω.

Concerning the first aspect we notice that, based on the points η_{ij} and on the aforementioned index sets, the grid points are positioned block–wise for the scale $l = 0$:

$${}^{00}B_k^{(0)} = \left\{ \eta_{2i+(2^k-1)\,j} \mid (i,j) \in \mathcal{I}_k^{(0)} \right\},\ k = 0, \ldots, N - 1. \tag{9}$$

Clearly, all grid points are collected in the set

$$ {}^{00}B^{(0)} = \bigcup_{k=0}^{N-1} {}^{00}B_k^{(0)}. \tag{10} $$

Figure 3 illustrates the sets for different N.

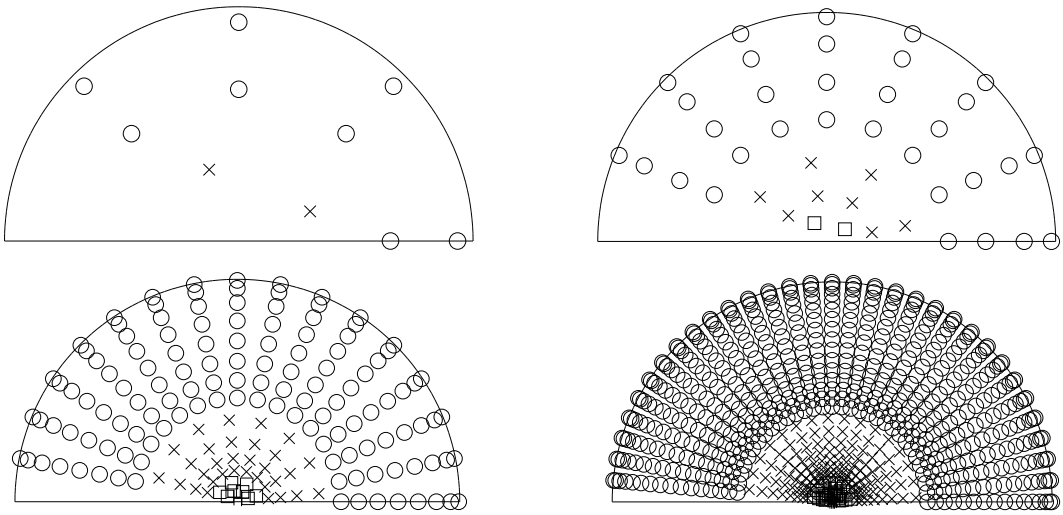

Figure 3: Point sets for $N = 2, 3, 4$, and 5. Block 0: o, block 1: $\times$, block 2: $\square$, block 3: $+$, block 4: $*$.

Our purpose now is to extend the grid to the whole sphere and to introduce a hierarchical structure. To this end we let

$$ {}^{00}\eta_{ij} = \eta_{ij} = \begin{pmatrix} \sin\vartheta_j \cos\lambda_i \\ \sin\vartheta_j \sin\lambda_i \\ \cos\vartheta_j \end{pmatrix}, \quad {}^{01}\eta_{ij} = \begin{pmatrix} \sin\vartheta_j \cos(\pi+\lambda_i) \\ \sin\vartheta_j \sin(\pi+\lambda_i) \\ \cos\vartheta_j \end{pmatrix}, \tag{11} $$

$$ {}^{10}\eta_{ij} = \begin{pmatrix} \sin(\pi-\vartheta_j) \cos\lambda_i \\ \sin(\pi-\vartheta_j) \sin\lambda_i \\ \cos(\pi-\vartheta_j) \end{pmatrix}, \quad {}^{11}\eta_{ij} = \begin{pmatrix} \sin(\pi-\vartheta_j) \cos(\pi+\lambda_i) \\ \sin(\pi-\vartheta_j) \sin(\pi+\lambda_i) \\ \cos(\pi-\vartheta_j) \end{pmatrix}, \tag{12} $$

In consequence, four blocks with indices $m, n \in \{0, 1\}$ are introduced by

$$ {}^{mn}B_k^{(l)} = \left\{ {}^{mn}\eta_{2i+(2^k-1)\,j} \;\middle|\; (i,j) \in \mathcal{I}_k^{(l)} \right\}. \tag{13} $$

Furthermore, we let

$$ {}^{mn}B^{(l)} = \bigcup_k {}^{mn}B_k^{(l)}. $$

By virtue of

$$ B^{(l)} = {}^{00}B^{(l)} \cup {}^{10}B^{(l)} \cup {}^{01}B^{(l)} \cup {}^{11}B^{(l)} $$

we obtain a block–structured set of points on the whole unit sphere.

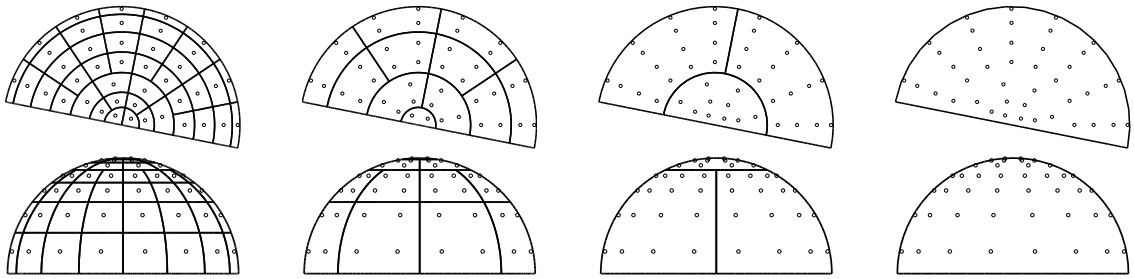

Figure 4: The SGS ${}^{00}S^{(l)}_{ij,k}$ for $N = 3$ and the scales 0,1,2,3 (from left to right). First row: Top view. Second row: Side view. The underlying point set is also shown.

Lemma 1 *For $N \geq 2$, the total number of points in the grid reads*

$$\#B^{(0)} = \frac{8}{3}(4^N - 1).$$

Next we come to the second aspect, i.e., the specification of SGS, which will help us later on to introduce, for each $(i, j) \in \mathcal{I}^{(l)}_k$, scaling and wavelet functions with suitably adapted local support. We understand for $m = n = 0$ the SGS ${}^{00}S^{(l)}_{ij,k}$ to be the rectangle (formulated in the framework of polar coordinates)

$${}^{00}S^{(l)}_{ij,k} = \left[(i - 1/2)2^{-N}\pi, (i + 2^{l+k} - 1/2)2^{-N}\pi\right] \times \left[\frac{1}{2}(\vartheta_j + \vartheta_{j-1}), \frac{1}{2}(\vartheta_{j+2l} + \vartheta_{j+2l-1})\right]. \quad (14)$$

This definition may fail at the boarders of the j–region. We therefore substitute in this definition for $j = 0$ the expression $\frac{1}{2}(\vartheta_j + \vartheta_{j-1})$ by $\pi/2$, and if $j + 2l > 2^N - 2$, we substitute the term $\frac{1}{2}(\vartheta_{j+2l} + \vartheta_{j+2l-1})$ by 0. For the other cases of $m, n \in \{0, 1\}$ we make similar definitions, but omit the details here. With this construction we associate with each scaling function a certain area of the unit sphere Ω, and we get, furthermore, a partition of Ω in the sets ${}^{mn}S^{(l)}_{ij,k}$ for each l. These associated supports are sketched for different l in Figure 4.

3 Scaling Function

The wavelet approach as discussed in this paper is discrete in space and scale. Our aim now is to describe the construction of the scaling function in accordance with the grid generated for a presribed N.

Obviously, the points in the set $B^{(0)}$ are arranged in $2^N - 1$ circles of latitude on the northern hemisphere and (symmetrically) in $2^N - 1$ circles on the southern hemisphere. As point of departure for our promised biorthogonalisation method we make the assumption that there are given $2^N - 1$ kernels $K_j \in \mathcal{L}^2[-1, 1]$, $j = 0, \ldots, 2^N - 2$ with local support $\mathrm{supp} K_j = [h_j, 1]$.

We furthermore suppose that

$$2\pi \int_{-1}^{1} K_j(t)dt = 1. \tag{15}$$

With these kernels we define, for the scale $l = 0$, the scaling functions to be

$${}^{mn}\varphi_{ij}^{(0)} = K_j({}^{mn}\eta_{2i+(2^k-1)\,j}\cdot\,), \quad (i,j) \in \mathcal{I}_k^{(l)}.$$

From (15) it is clear that

$$\int_{\Omega} {}^{mn}\varphi_{ij}^{(0)}(\xi)d\omega(\xi) = 1.$$

The scaling function for the scale $l = 0$ are zonal kernel functions on the sphere. Consequently they are an appropriate tool for problems of geomathematics, which can be formulated using rotation–invariant pseudodifferential operators (see, e.g., [8] and the references therein).

The support of the scaling function at scale $l = 0$ (for example, if $m = n = 0$) is

$$\mathrm{supp}^{00}\varphi_{ij}^{(0)} = \left\{\eta \in \Omega \mid \eta \cdot \eta_{2i+(2^k-1)\,j} \geq h_j\right\},$$

where the parameter h_j has to be chosen in close adaption to the associated SGS.

In addition, we assume that there is a second set of locally supported kernels $\tilde{K}_j \in \mathcal{L}^2[-1,1]$, $j = 0,\ldots,2^N-2$ with local support $\mathrm{supp}\tilde{K}_j = [h_j,1]$ and $2\pi\int_{-1}^{1}\tilde{K}_j(t)dt = 1$.

Finally, by taking

$${}^{mn}\tilde{\varphi}_{ij}^{(0)} = \tilde{K}_j({}^{mn}\eta_{2i+(2^k-1)\,j}\cdot\,), \quad (i,j) \in \mathcal{I}_k^{(l)}, \tag{16}$$

we are led to a biorthogonal system satisfying

$$({}^{mn}\varphi_{ij}^{(0)}, {}^{m'n'}\tilde{\varphi}_{i'j'}^{(0)}) = \delta_{ii'}\delta_{jj'}\delta_{mm'}\delta_{nn'}, \tag{17}$$

where $(\cdot,\cdot)$ is the $\mathcal{L}^2(\Omega)$–inner product.

Note that the appropriate kernels $\tilde{K}_j$ can be constructed from the given kernels K_j (or vice versa). The numerical effort is small: For each j a linear system of equations has to be solved. For typical applications, these systems have about 10–20 equations, dependent on the supports $[h_j,1]$. Details can be found in a forthcoming paper [14].

In other words, a primal scaling function together with its dual counterpart are defined for the scale $l = 0$ with respect to the grid $B^{(0)}$. It remains to construct the scaling functions for the other scales. We do this successively: Assume, ${}^{mn}\varphi_{ij}^{(l-1)}$ and ${}^{mn}\tilde{\varphi}_{ij}^{(l-1)}$ are already given. Then we set for $k = 0,\ldots,N-l-1$ and $m,n \in \{0,1\}$ and $(i,j) \in \mathcal{I}_k^{(l)}$

$${}^{mn}\varphi_{ij}^{(l)} = \frac{1}{2}\left({}^{mn}\varphi_{ij}^{(l-1)} + {}^{mn}\,\varphi_{i+2^{k+l-1}\,j}^{(l-1)} + {}^{mn}\,\varphi_{i\,j+2^{l-1}}^{(l-1)} + {}^{mn}\,\varphi_{i+2^{k+l-1}\,j+2^{l-1}}^{(l-1)}\right). \tag{18}$$

For $k = N-l$ we have to distinguish two cases. If $l = 1$,

$${}^{mn}\varphi_{ij}^{(l)} = \frac{1}{\sqrt{2}}\left({}^{mn}\varphi_{ij}^{(l-1)} + {}^{mn}\,\varphi_{i+2^{k+l-1}\,j}^{(l-1)}\right) \tag{19}$$

and if $l \neq 1$

$$ {}^{mn}\varphi_{ij}^{(l)} = \frac{1}{2}\left({}^{mn}\varphi_{ij}^{(l-1)} + {}^{mn}\varphi_{i+2^{k+l-1}\,j}^{(l-1)} + 2\,{}^{mn}\varphi_{i\,j+2^{l-1}}^{(l-1)} \right) \tag{20} $$

for $(i,j) \in \mathcal{I}_k^{(l)}$. The idea of this construction is as follows: The scaling function is the mean of the four scaling functions corresponding to four neighboring indices. This construction works if the four points belong to one block. Of course, the other cases (i.e., $k = N - l$) have to be considered, when only two scaling functions are in a block. Then the mean is formed with the two scaling functions of this block and the scaling function of the neighboring block (in direction to the pole). In this neighboring block there is (at this stage) only one point. The situation with $l = 1$ is given only for the first scale, when in the block ${}^{mn}B_{N-1}^{(0)}$ are two points and the block ${}^{mn}B_N^{(0)}$ does not exist.

The dual scaling functions are defined similarly. We set for $k = 1, \ldots, N - l$ and $m, n \in \{0, 1\}$ and $(i,j) \in \mathcal{I}_k^{(l)}$

$$ {}^{mn}\tilde{\varphi}_{ij}^{(l)} = \frac{1}{2}\left({}^{mn}\tilde{\varphi}_{ij}^{(l-1)} + {}^{mn}\tilde{\varphi}_{i+2^{k+l-1}\,j}^{(l-1)} + {}^{mn}\tilde{\varphi}_{i\,j+2^{l-1}}^{(l-1)} + {}^{mn}\tilde{\varphi}_{i+2^{k+l-1}\,j+2^{l-1}}^{(l-1)} \right). \tag{21} $$

For $k = N - l + 1$ we have to distinguish two cases, again. If $l = 1$,

$$ {}^{mn}\tilde{\varphi}_{ij}^{(l)} = \frac{1}{\sqrt{2}}\left({}^{mn}\tilde{\varphi}_{ij}^{(l-1)} + {}^{mn}\tilde{\varphi}_{i+2^{k+l-1}\,j}^{(l-1)} \right) \tag{22} $$

and if $l \neq 1$

$$ {}^{mn}\tilde{\varphi}_{ij}^{(l)} = \frac{1}{2}\left({}^{mn}\tilde{\varphi}_{ij}^{(l-1)} + {}^{mn}\tilde{\varphi}_{i+2^{k+l-1}\,j}^{(l-1)} + 2\,{}^{mn}\tilde{\varphi}_{i\,j+2^{l-1}}^{(l-1)} \right) \tag{23} $$

for $(i,j) \in \mathcal{I}_k^{(l)}$.

With this construction of the scaling function and the dual scaling function we get for each scale a biorthogonal system

Theorem 2 *For each scale l,*

$$ ({}^{mn}\varphi_{ij}^{(l)}, {}^{m'n'}\tilde{\varphi}_{i'j'}^{(l)})_{\mathcal{L}^2(\Omega)} = \delta_{ii'}\delta_{jj'}\delta_{mm'}\delta_{nn'}. $$

For higher scales, the support of a scaling function obviously is the union of the supports of the scaling function which it is built with. Once more, it is helpful to associate for each scaling function a SGS with respect to the underlying grid as defined before.

4 Wavelets

The scaling functions introduced in the last section enable us to define a particular concept of wavelets. Of course, wavelets correspond to a scale $l = 1, \ldots, N$ and to an area of Ω, which is

associated to $(i,j) \in \mathcal{I}_k^{(l)}$. We set for $k = 1, \ldots, N-l-1$, $m,n \in \{0,1\}$ and $(i,j) \in \mathcal{I}_k^{(l)}$,

$$
\begin{aligned}
{}^{mn}_{EW}\psi_{ij}^{(l)} &= \frac{1}{2}\left({}^{mn}\varphi_{ij}^{(l-1)} - {}^{mn}\varphi^{(l-1)}_{i+2^{k+l-1}\,j} + {}^{mn}\varphi^{(l-1)}_{i\,j+2^{l-1}} - {}^{mn}\varphi^{(l-1)}_{i+2^{k+l-1}\,j+2^{l-1}}\right), && (24)\\
{}^{mn}_{NS}\psi_{ij}^{(l)} &= (-1)^m\frac{1}{2}\left({}^{mn}\varphi_{ij}^{(l-1)} + {}^{mn}\varphi^{(l-1)}_{i+2^{k+l-1}\,j} - {}^{mn}\varphi^{(l-1)}_{i\,j+2^{l-1}} - {}^{mn}\varphi^{(l-1)}_{i+2^{k+l-1}\,j+2^{l-1}}\right), && (25)\\
{}^{mn}_{D}\psi_{ij}^{(l)} &= (-1)^m\frac{1}{2}\left({}^{mn}\varphi_{ij}^{(l-1)} - {}^{mn}\varphi^{(l-1)}_{i+2^{k+l-1}\,j} - {}^{mn}\varphi^{(l-1)}_{i\,j+2^{l-1}} + {}^{mn}\varphi^{(l-1)}_{i+2^{k+l-1}\,j+2^{l-1}}\right). && (26)
\end{aligned}
$$

As already pointed out, the suffixes EW, NS, and D stand for east–west, north–south and diagonal. Thus the idea of this framework should become clear: The differences between the scaling function ${}^{mn}\varphi_{ij}^{(l)}$ and its four constituting blocks are transcribed to three wavelets. One corresponds to the east–west structure, one stands for the north–south structure, and one is of mixed type. The factor $(-1)^m$ is due to the fact, that on the southern hemisphere, the point sets are generated by mirroring the sets from the northern hemisphere at the equator. Thus, the role of north and south is changed, and this is compensated with the factor -1 on the southern hemisphere.

As for the scaling function we have to consider the special case $k = N-l$ separately. Analogously to the scaling function, for $k = N-l$, we let

$$
{}^{mn}_{EW}\psi_{ij}^{(l)} = \frac{1}{\sqrt{2}}\left({}^{mn}\varphi_{ij}^{(l-1)} - {}^{mn}\varphi^{(l-1)}_{i+2^{k+l-1}\,j}\right) \tag{27}
$$

if $l = 1$ and, if $l \neq 1$

$$
\begin{aligned}
{}^{mn}_{EW}\psi_{ij}^{(l)} &= \frac{1}{\sqrt{2}}\left({}^{mn}\varphi_{ij}^{(l-1)} - {}^{mn}\varphi^{(l-1)}_{i+2^{k+l-1}\,j}\right), && (28)\\
{}^{mn}_{NS}\psi_{ij}^{(l)} &= (-1)^m\frac{1}{2}\left({}^{mn}\varphi_{ij}^{(l-1)} + {}^{mn}\varphi^{(l-1)}_{i+2^{k+l-1}\,j} - 2\,{}^{mn}\varphi^{(l-1)}_{i\,j+2^{l-1}}\right). && (29)
\end{aligned}
$$

Using the same formulas (with $\tilde{\varphi}$ instead of φ), the dual wavelets $\tilde{\psi}$ are definable. As an immediate consequence of this construction we find

Lemma 3 *Each wavelet ${}^{mn}_{X}\psi_{ij}^{(l)}$ and each dual wavelet ${}^{mn}_{X}\tilde{\psi}_{ij}^{(l)}$, $X \in \{EW, NS, D\}$, is a linear combination of zonal functions. Furthermore, the zero mean property is valid:*

$$
\int_\Omega {}^{mn}_{X}\psi_{ij}^{(l)}(\xi)\,d\omega(\xi) = \int_\Omega {}^{mn}_{X}\tilde{\psi}_{ij}^{(l)}(\xi)\,d\omega(\xi) = 0.
$$

Our considerations provide us with a biorthogonal system of both scaling and wavelet functions:

Theorem 4 *The sets*

$$
\{{}^{00}\varphi_{ij}^{(N)}, {}^{01}\varphi_{ij}^{(N)}, {}^{10}\varphi_{ij}^{(N)}, {}^{11}\varphi_{ij}^{(N)}\} \cup \{{}^{mn}_{X}\psi_{ij}^{(l)} \mid \text{when available}\}
$$

and

$$
\{{}^{00}\tilde{\varphi}_{ij}^{(N)}, {}^{01}\tilde{\varphi}_{ij}^{(N)}, {}^{10}\tilde{\varphi}_{ij}^{(N)}, {}^{11}\tilde{\varphi}_{ij}^{(N)}\} \cup \{{}^{mn}_{X}\tilde{\psi}_{ij}^{(l)} \mid \text{when available}\}
$$

form a biorthogonal system.

It should be noted that our approach leads us to a different number of wavelets (EW, NS, and D) for varying indices (i, j) from scale to scale.

An illustration of the results of our construction is given in Figure 5.

Scale (l)	Blocks (k)	Wavelet Types EW	NS	D
$l = 1$	$k = 0, 1, \ldots, N-2$	$\times$	$\times$	$\times$
	$k = N-1$	$\times$		
$l = 2, \ldots, N$	$k = 0, \ldots, N-l-1$	$\times$	$\times$	$\times$
	$k = N-1$	$\times$	$\times$	

Figure 5: Available wavelet types for different scales and blocks.

5 Multiresolution Analysis

Once again, suppose that $N \geq 2$ is fixed, and the scaling and wavelet functions are defined in accordance with our approach. For $l = 0, \ldots, N$ we introduce the scale space V_l as the span of all functions ${}^{mn}\tilde{\varphi}_{ij}^{(0)}$ for $k = 0, \ldots, N-1,\ (i,j) \in \mathcal{I}_k^{(0)},\ m, n \in \{0, 1\}$, i.e., we let

$$V_0 = \left\langle {}^{mn}\tilde{\varphi}_{ij}^{(0)} \ \middle| k = 0, \ldots, N-1,\ (i,j) \in \mathcal{I}_k^{(0)},\ m, n \in \{0,1\} \right\rangle, \tag{30}$$

and for $l = 1, \ldots, N$

$$V_l = \left\langle {}^{mn}\tilde{\varphi}_{ij}^{(l)} \ \middle| k = 0, \ldots, N-l,\ (i,j) \in \mathcal{I}_k^{(l)},\ m, n \in \{0,1\} \right\rangle. \tag{31}$$

These finite dimensional spaces possess the dimension

$$\dim V_l = \frac{8}{3}(4^{N-l} - 1) + 4(1 - \delta_{l0}). \tag{32}$$

Moreover, they form a nested sequence of subspaces in the form

$$\{0\} \subset V_N \subset V_{N-1} \subset \ldots \subset V_1 \subset V_0 \subset \mathcal{L}^2(\Omega). \tag{33}$$

Observing the property of biorthogonality for the scaling function we are able to define projection operators $P_l : \mathcal{L}^2(\Omega) \longrightarrow V_l$ by

$$P_l(F) = \sum_{k,m,n} \sum_{(i,j) \in \mathcal{I}_k^{(l)}} ({}^{mn}\varphi_{ij}^{(l)}, F)\, {}^{mn}\tilde{\varphi}_{ij}^{(l)}, \tag{34}$$

where, as always, $(\cdot, \cdot)$ is understood in the topology of $\mathcal{L}^2(\Omega)$. It is clear, that $P_l(F) = F$ whenever $F \in V_l$. In the sense of signal processing, the projection operators P_l can be associated with low–pass filtering.

The difference between two succeeding scale spaces is collected in a detail space. In more detail, we define

$$W_1 = \left\langle {}^{mn}_{X}\tilde{\psi}^{(1)}_{ij} \;\middle|\; k = 0, \ldots, N-2,\ (i,j) \in \mathcal{I}^{(1)}_k,\ m,n \in \{0,1\},\ X \in \{EW, NS, D\} \right\rangle \\ \oplus \left\langle {}^{mn}_{EW}\tilde{\psi}^{(1)}_{ij} \;\middle|\; (i,j) \in \mathcal{I}^{(1)}_{N-1},\ m,n \in \{0,1\} \right\rangle. \tag{35}$$

while, for $l = 2, \ldots, N$, we let

$$W_l = \left\langle {}^{mn}_{X}\tilde{\psi}^{(l)}_{ij} \;\middle|\; k = 0, \ldots, N-l-1,\ (i,j) \in \mathcal{I}^{(l)}_k,\ m,n \in \{0,1\},\ X \in \{EW, NS, D\} \right\rangle \\ \oplus \left\langle {}^{mn}_{X}\tilde{\psi}^{(l)}_{ij} \;\middle|\; (i,j) \in \mathcal{I}^{(l)}_{N-l},\ m,n \in \{0,1\},\ X \in \{EW, NS\} \right\rangle. \tag{36}$$

In doing so we get $\dim W_l = 2\ 4^{N-l+1} - 4\delta_{l1}$. Furthermore, because of the decomposition of V_{l-1} as direct sum of W_l and V_l, i.e.,

$$W_l \oplus V_l = V_{l-1},\ l = 1, \ldots, N, \tag{37}$$

we are able to deduce

Lemma 5 *For $N \geq 2$ fixed,*

$$V_0 = V_N \oplus \bigoplus_{l=1}^{N} W_l.$$

The space W_l contains the detail information of a signal F. In fact, our method enables a dynamical space-varying frequency distribution of a function $F \in \mathcal{L}^2(\Omega)$. Consequently, the wavelet analysis is not only related to a frequency band (according to the scale l), but also scale–dependent spatial information is provided.

The analysis is performed by the wavelets transform, that is defined as follows: For the scale l and the index $(i,j) \in \mathcal{I}^{(l)}_k$,

$${}^{mn}_{X}\mathrm{WT}(l;i,j;F) = ({}^{mn}_{X}\psi^{(l)}_{ij}, F),\ F \in \mathcal{L}^2(\Omega), \tag{38}$$

where $m,n \in \{0,1\}$ and $X \in \{EW, NS, D\}$ (when defined). Due to the biorthogonality of the wavelets and the dual wavelets, we are able to introduce the operators $R_l : \mathcal{L}^2(\Omega) \longrightarrow W_l$ by

$$R_l(F) = \sum_{k,m,n} \sum_{(i,j) \in \mathcal{I}^{(l)}_k} \sum_{X \in \{EW,NS,D\}} ({}^{mn}_{X}\psi^{(l)}_{ij}, F)\ {}^{mn}_{X}\tilde{\psi}^{(l)}_{ij}. \tag{39}$$

These operators act as band–pass filters on a signal $F \in \mathcal{L}^2(\Omega)$.

The wavelet analysis and the reconstruction can be summarized in the following

Theorem 6 *For $F \in \mathcal{L}^2(\Omega)$,*

$$P_0(F) = \sum_{m,n\in\{0,1\}} \left(({}^{mn}\varphi_{00}^{(N)}, F)\, {}^{mn}\tilde{\varphi}_{00}^{(n)} + \sum_{l=1}^{N} \sum_{k} \sum_{(i,j)\in\mathcal{I}_k^{(l)}} \sum_{X\in\{EW,NS,D\}} ({}^{mn}_{X}\psi_{ij}^{(l)}, F)\ {}^{mn}_{X}\tilde{\psi}_{ij}^{(l)} \right).$$

The wavelet analysis and the reconstruction can be organized as a fast wavelet transform. Basis for this algorithms are the filter coefficients in the scale relation, which are implicitly defined in (18)–(29). For example, it follows from (24) that

$$\begin{gathered} {}^{mn}_{EW}\mathrm{WT}(l;i,j;F) = \\ \tfrac{1}{2}\left(({}^{mn}\varphi_{ij}^{(l-1)}, F) - ({}^{mn}\varphi_{i+2^{k+l-1}\,j}^{(l-1)}, F) + ({}^{mn}\varphi_{i\,j+2^{l-1}}^{(l-1)}, F) - ({}^{mn}\varphi_{i+2^{k+l-1}\,j+2^{l-1}}^{(l-1)}, F)\right). \end{gathered}$$

In fact, we end up with a fast tree algorithm of the following structure:

Wavelet Decomposition

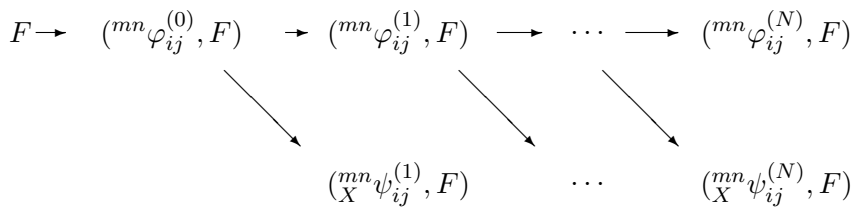

The reconstruction can be organized as follows:

Wavelet Reconstruction

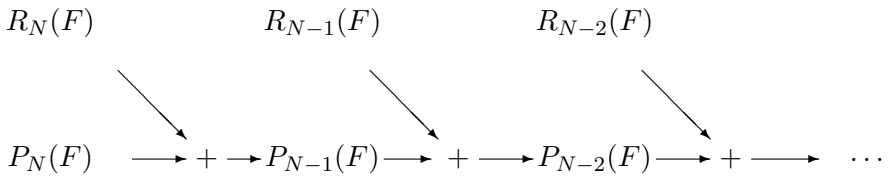

6 Examples

We present two examples for the described wavelet approach. The first example shows a function $F \in \mathcal{L}^2(\Omega)$ consisting of two spherical harmonics of degree 4, a zonal one and a tesseral one. We choose the example in such a way that there is a discontinuity along a circle of latitude (cf. Figure 6).

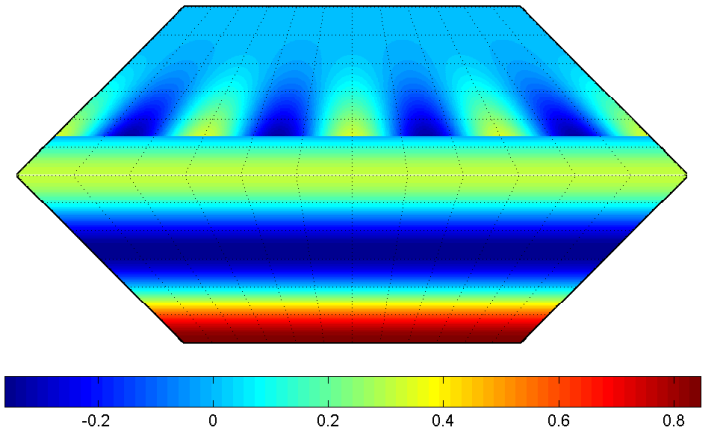

Figure 6: The function F built out of two spherical harmonics.

The point set is constituted with $N = 8$, that is, we have a pointset with approximately 87000 points. Since the pointset is rather dense for this function, we decided to approximate $({}^{mn}\varphi_{ij}^{(0)}, F)$ just by the value $F({}^{mn}\eta_{2i+(2^k-1)})$. This is an efficient approach, when the data are dense enough. The wavelet transforms are then calculated using the algorithms described in the last chapter. The wavelet transforms of types east–west and north–south are presented in Figure 7. For this, we plotted each SGS with a color specified by the corresponding wavelet transform. The wavelet transform at scale j is multiplied with a factor 2^{-j} to get comparable results.

As a second example, we take a test function composed by an Abel–Poisson kernel located at the southern hemisphere and by two singularity kernels at the northern hemisphere (cf. [8]). The parameters of the singularity kernels are set in such a way, that they are associated with the gravitational potential of buried point masses with different depths. The function is illustrated in Figure 8. The function is sampled at a grid ($N = 9$) with approximately 700.000 points. Again, we approximated the integrals for the finest scale by functional values. The wavelet transforms at different scales are presented in Figure 9.

7 Conclusions

The paper is motivated as follows: In the context of physical geodesy and space physics, a large number of observables of the gravity field can be represented by rotation–invariant pseudodifferential operators applied to the Earth's disturbing potential (for example, gravity anomaly, geoid undulation, first and second radial derivative of the disturbance potential obtained by satellite–to–satellite tracking and/or satellite gravity gradiometry). Moreover, at least when low earth orbiters (such as the satellites GRACE, CHAMP, and GOCE) come into play we are confronted with millions of data distributed over dense structured grids. In consequence, the problem of modeling spaceborne data requires the determination of the Earth's gravity

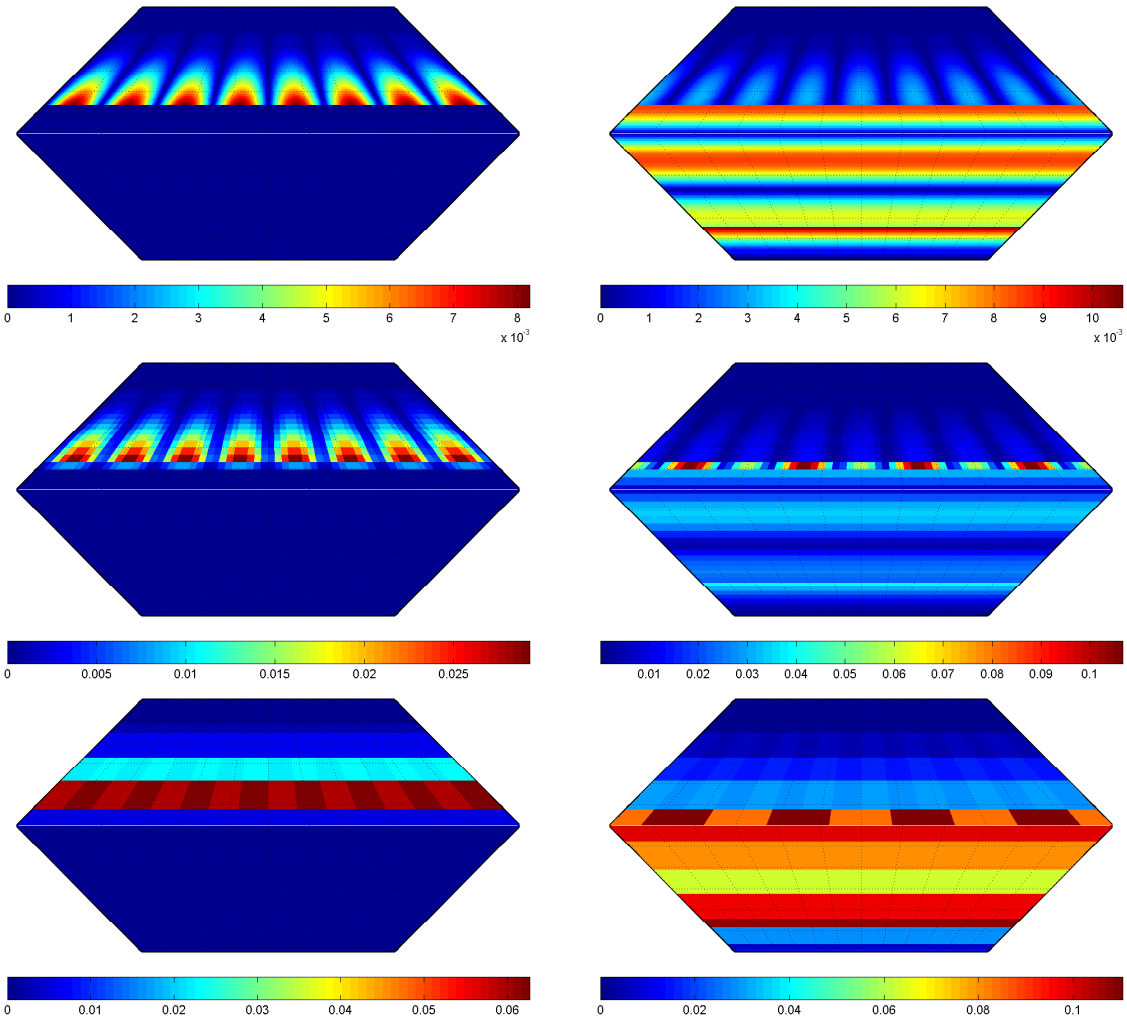

Figure 7: The values of the wavelet transforms (east–west on the left hand side, north–south on the right hand side). Shown are the scales 1, 3, and 5.

potential by an efficient and economical evaluation procedure for dense data structures. At the same time, the comparability of the different observables of isotropic character should be available in a unified setup.

Our approach fills up this gap by formulating a fast wavelet transform on spherical reference surfaces under the geophysical relevant assumption of isotropy. In addition, when dealing with satellite data there is a strong need for regularization, i.e., downward continuation by means of inverse Abel–Poisson–type operators (see, [8], [7], [17], [27]). Since these operators also are rotational invariant pseudodifferential operators, downward continuation of satellite data, indeed, becomes attackable by our fast wavelet implementation involving zonal kernel functions. Because of the space localizing properties of the scaling and wavelet functions, our method enables fast approximations of local phenomena, too. Even more, it should be

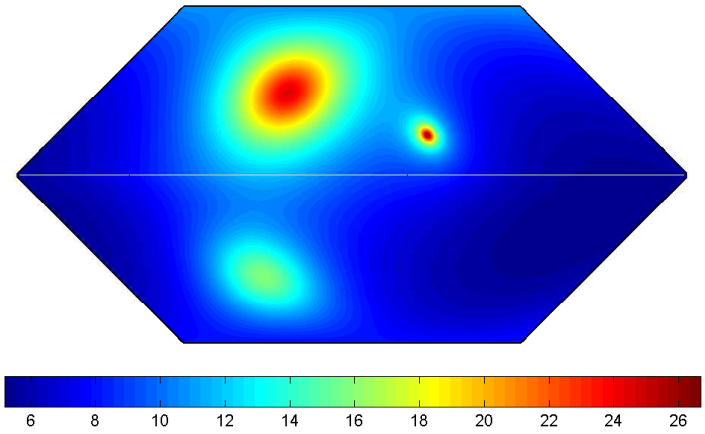

Figure 8: The function F built out of an Abel–Poisson kernel and two singularity kernels centered at in the northern hemisphere.

mentioned that it is possible to apply the described concept in a fully local framework.

References

[1] Antoine, J.-P., Demanet, L., Jaques, L., Vandergheynst, P. (2002). Wavelets on the Sphere: Implementations and Approximations, *Appl. Comput. Harmon. Anal.*, **13**, 177-200.

[2] Antoine, J.-P., Vandergheynst, P. (1999). Wavelets on the 2–sphere: A Group–theoretic Approach, *Appl. Comp. Harmon. Anal.*, **7**, 1-30.

[3] Bauer, F., Freeden, W., Schreiner, M. (2006). A Tree Algorithm for Isotropic Finite Elements on the Sphere, *Numer. Funct. Anal. Optim.*, **27**, 1-24.

[4] Bayer, M. (2000). Geomagnetic Field Modelling From Satellite Data by First and Second Generation Wavelets, *PhD–thesis, University of Kaiserslautern, Geomathematics Group, Shaker, Aachen.*

[5] Dahlke, S., Dahmen, W., Schmitt, E., Weinreich, I. (1995). Multiresolution Analysis and Wavelets on S^2 and S^3, *Numer. Funct. Anal. Optimiz.*, **16**(1&2), 19-41.

[6] Dahlke, S., Maass, P. (1996). Continuous Wavelet Transforms with Applications to Analyzing Functions on Spheres, *J. Fourier Anal. Appl.*, **2**(4), 379–396.

[7] Freeden, W. (1999). Multiscale Modelling of Spaceborne Geodata, *B.G. Teubner, Stuttgart, Leipzig.*

[8] Freeden, W., Gervens, T., Schreiner, M. (1998). Constructive Approximation on the Sphere (With Applications to Geomathematics), *Oxford Science Publications, Clarendon.*

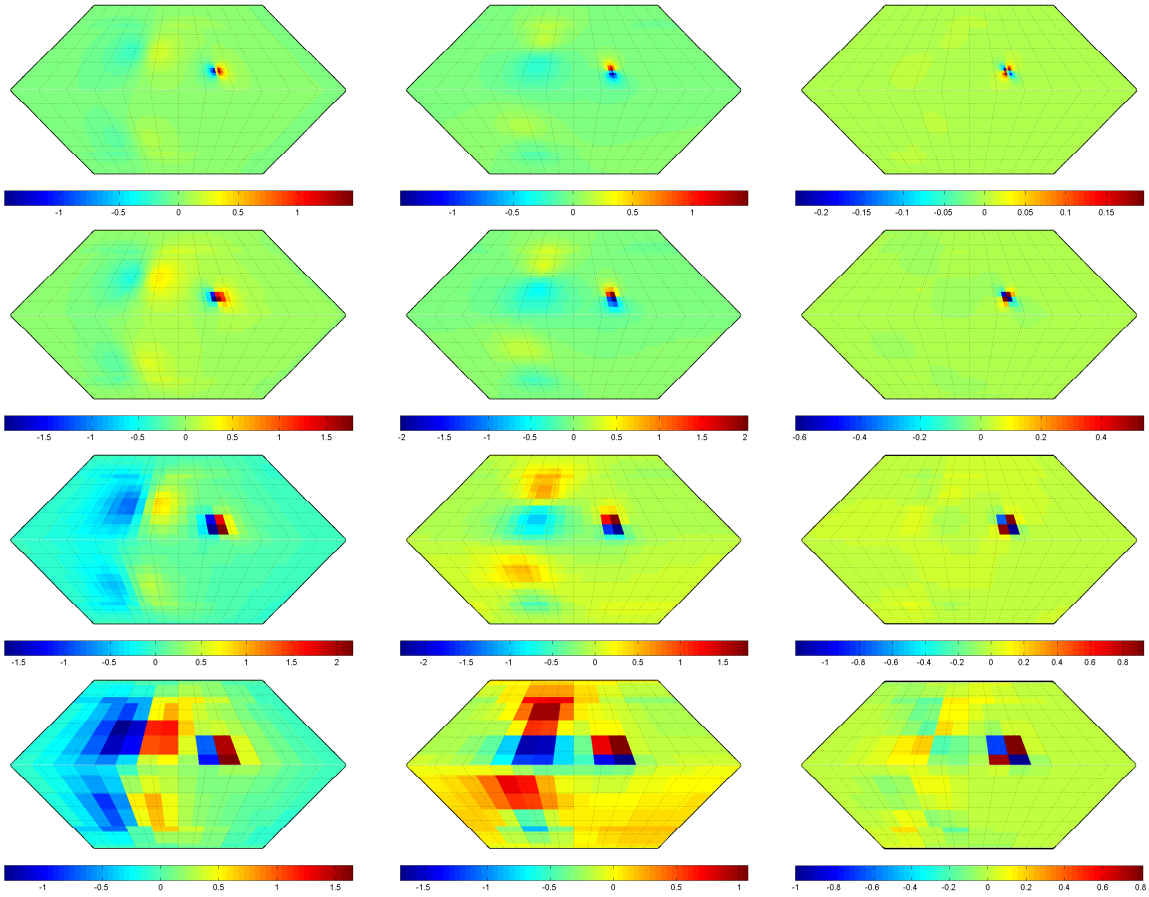

Figure 9: The values of the wavelet transforms (east–west, north–south, and diagonal). Shown are the scales 3, 4, 5, and 6.

[9] Freeden, W., Hesse, K. (2002). On the Multiscale Solution of Satellite Problems by Use of Locally Supported Kernel Functions Corresponding to Equidistributed Data on Spherical Orbits, *Stud. Sci. Math. Hung.*, **39**, 37-74.

[10] Freeden, W., Maier, T. (2002). On Multiscale Denoising of Spherical Functions: Basic Theory and Numerical Aspects, *Electron. Trans. Numer. Anal.*, **14**, 40-62.

[11] Freeden, W., Mayer, C. (2003). Wavelets Generated by Layer Potentials, *Appl. Comput. Harmon. Anal.*, **14**, 195-237.

[12] Freeden, W., Mayer, C., Schreiner, M. (2003). Tree Algorithms in Wavelet Approximation by Helmholtz Potential Operators, *Numer. Funct. Anal. Optim.*, **24**, 747-782.

[13] Freeden, W., Michel, V. (2004). Multiscale Potential Theory (With Applications to Geoscience). *Birkhäuser, Boston, Basel, Berlin.*

[14] Freeden, W., Moghiseh, A., Schreiner, M. (2006). Biorthogonalization on the Sphere Made Simple (In Preparation).

[15] Freeden, W., Schreiner, M. (1995). Non–orthogonal Expansions on the Sphere, *Math. Meth. in the Appl. Sci.*, **18**, 83-120.

[16] Freeden, W., Schreiner, M. (1997). Orthogonal and Non-orthogonal Multiresolution Analysis, Scale Discrete and Exact Fully Discrete Wavelet Transform on the Sphere, *Constr. Approx.*, **14**, 493-515.

[17] Freeden, W., Schreiner, M. (2005). Spaceborne Gravitational Field Determination by Means of Locally Supported Wavelets, *Journal of Geodesy*, **79**, 431-446.

[18] Freeden, W., Schreiner, M. (2006). Multiresolution Analysis by Spherical Up Functions, *Constr. Approx.* **23**, 241-259.

[19] Freeden, W., Windheuser, U. (1996). Spherical Wavelet Transform and Its Discretization, *Adv. Comput. Math.,* **5**, 51-94.

[20] Freeden, W., Windheuser, U. (1997). Combined Spherical Harmonic and Wavelet Expansion — A Future Concept in Earth's Gravitational Determination, *Appl. Comput. Harm. Anal.*, **4**, 1-37.

[21] Holschneider, M. (1996). Continuous Wavelet Transforms on the Sphere, *J. Math. Phys.*, **37**, 4156-4165.

[22] Louis, A. K., Maass, P., Rieder, A. (1998). Wavelets: Theorie und Anwendungen. Teubner Studienbücher Mathematik, *B.G. Teubner, Stuttgart.*

[23] Lyche, T., Schumaker, L. (2000). A Multiresolution Tensor Spline Method for Fitting Functions on the Sphere, *SIAM J. Sci. Comput.*, **22**, 724-746.

[24] Potts, D., Tasche, M. (1995). Interpolatory Wavelets on the Sphere, in: C.K. Chui, L.L. Schumaker, eds. *Approximation Theory VIII, World Scientific, Singapore*, 335-342.

[25] Schreiner, M. (1996). A Pyramid Scheme for Spherical Wavelets, *AGTM Report, No. 170, University of Kaiserslautern, Geomathematics Group.*

[26] Schreiner, M. (1997). Locally Supported Kernels for Spherical Spline Interpolation, *J. Approx. Theory*, **89**, 172-194.

[27] Schreiner, M. (2004). Wavelet Approximation by Spherical Up Functions, *Habilitation–thesis, University of Kaiserslautern, Geomathematics Group, Shaker, Aachen.*

[28] Schröder, P., Sweldens, W. (1995). Spherical Wavelets: Efficiently Representing Functions on the Sphere, in: *Computer Graphics Proceedings (SIGGRAPH95),* 161-175.

[29] Weinreich, I. (2001). A Construction of $C^{(1)}$–wavelets on the Two–dimensional Sphere, *Appl. Comput. Harmon. Anal.*, **10**, 1-26.

Folgende Berichte sind erschienen:

2003

Nr. 1 S. Pereverzev, E. Schock.
On the adaptive selection of the parameter in regularization of ill-posed problems

Nr. 2 W. Freeden, M. Schreiner.
Multiresolution Analysis by Spherical Up Functions

Nr. 3 F. Bauer, W. Freeden, M. Schreiner.
A Tree Algorithm for Isotropic Finite Elements on the Sphere

Nr. 4 W. Freeden, V. Michel (eds.)
Multiscale Modeling of CHAMP-Data

Nr. 5 C. Mayer
Wavelet Modelling of the Spherical Inverse Source Problem with Application to Geomagnetism

2004

Nr. 6 M.J. Fengler, W. Freeden, M. Gutting
Darstellung des Gravitationsfeldes und seiner Funktionale mit Multiskalentechniken

Nr. 7 T. Maier
Wavelet-Mie-Representations for Soleniodal Vector Fields with Applications to Ionospheric Geomagnetic Data

Nr. 8 V. Michel
Regularized Multiresolution Recovery of the Mass Density Distribution From Satellite Data of the Earth's Gravitational Field

Nr. 9 W. Freeden, V. Michel
Wavelet Deformation Analysis for Spherical Bodies

Nr. 10 M. Gutting, D. Michel (eds.)
Contributions of the Geomathematics Group, TU Kaiserlautern, to the 2nd International GOCE User Workshop at ESA-ESRIN Frascati, Italy

Nr. 11 M.J. Fengler, W. Freeden
A Nonlinear Galerkin Scheme Involving Vector and Tensor Spherical Harmonics for Solving the Incompressible Navier-Stokes Equation on the Sphere

Nr. 12 W. Freeden, M. Schreiner
Spaceborne Gravitational Field Determination by Means of Locally Supported Wavelets

Nr. 13 F. Bauer, S. Pereverzev
Regularization without Preliminary Knowledge of Smoothness and Error Behavior

Nr. 14 W. Freeden, C. Mayer
Multiscale Solution for the Molodensky Problem on Regular Telluroidal Surfaces

Nr. 15 W. Freeden, K. Hesse
Spline modelling of geostrophic flow: theoretical and algorithmic aspects

2005

Nr. 16 M.J. Fengler, D. Michel, V. Michel
Harmonic Spline-Wavelets on the 3-dimensional Ball and their Application to the Reconstruction of the Earth's Density Distribution from Gravitational Data at Arbitrarily Shape Satellite Orbits

Nr. 17 F. Bauer
Split Operators for Oblique Boundary Value Problems

Nr. 18 W. Freeden, M. Schreiner
Local Multiscale Modelling of Geoidal Undulations from Deflections of the Vertical

Nr. 19 W. Freeden, D. Michel, V. Michel
Local Multiscale Approximations of Geostrophic Flow: Theoretical Background and Aspects of Scientific Computing

Nr. 20 M.J. Fengler, W. Freeden, M. Gutting
The Spherical Bernstein Wavelet

Nr. 21 M.J. Fengler, W. Freeden,
A. Kohlhaas, V. Michel, T. Peters
Wavelet Modelling of Regional and Temporal Variations of the Earth's Gravitational Potential Observed by GRACE

Nr. 22 W. Freeden, C. Mayer
A Wavelet Approach to Time-Harmonic Maxwell's Equations

Nr. 23 M.J. Fengler, D. Michel, V. Michel
Contributions of the Geomathematics Group to the GAMM 76th Annual Meeting

Nr. 24 F. Bauer
Easy Differentiation and Integration of Homogeneous Harmonic Polynomials

Nr. 25 T. Raskop, M. Grothaus
On the Oblique Boundary Problem with a Stochastic Inhomogeneity

2006

Nr. 26 P. Kammann, V. Michel
Time-Dependent Cauchy-Navier Splines and their Application to Seismic Wave Front Propagation

Nr. 27 W. Freeden, M. Schreiner
Biorthogonal Locally Supported Wavelets on the Sphere Based on Zonal Kernel Functions

TECHNISCHE UNIVERSITÄT
KAISERSLAUTERN

Informationen:

Prof. Dr. W. Freeden
Prof. Dr. E. Schock
Fachbereich Mathematik
Technische Universität Kaiserslautern
Postfach 3049
D-67653 Kaiserslautern
E-Mail: freeden@mathematik.uni-kl.de
schock@mathematik.uni-kl.de